

Understanding and Controlling the Growth of Monodisperse CdS Nanowires in Solution

Lifei Xi,[†] Winnie Xiu Wen Tan,[†] Chris Boothroyd,[‡] and Yeng Ming Lam^{*†}

School of Materials Science and Engineering, Nanyang Technological University, Nanyang Avenue, Singapore 639798, and Center for Electron Nanoscopy, Technical University of Denmark, DK-2800 Kongens Lyngby, Denmark

Received May 26, 2008. Revised Manuscript Received June 24, 2008

Cadmium sulfide (CdS) nanowires with a monodisperse diameter of 3.5 nm and length of about 600 nm were successfully synthesized using a simple and reproducible hot coordination solvents method. Structural characterization showed that the one-dimensional nanowires grow along the [001] direction and have the wurtzite structure. The morphology of the nanocrystals is affected by the octadecylphosphonic acid to cadmium (ODPA-to-Cd) mole ratio, the precursor ratio (Cd-to-S mole ratio), the precursor concentration, the precursor injection process, and the type of ligands used in the synthesis. However, we propose that the ODPA-to-Cd mole ratio is the key factor affecting the morphology of the nanowires because it affects both the cleavage rate of the P=S double bond and the nucleation/growth rate of the anisotropic nanocrystals. In addition, it was found that Cd-ODPA complexes give rise to a low diffusion rate of the precursor and hence low reactivity. Therefore, ODPA is good for generating nearly monodisperse and high aspect ratio CdS nanowires. Our nanowires have a high degree of dispersibility and thus can be easily processed for potential applications as solar cells and transistors. Finally, the potential applications of these highly dispersible and high aspect ratio nanowires will also be discussed.

Introduction

Semiconductor nanowires exhibit physical properties that make them attractive building blocks for electronic, optical, and life sciences applications.^{1–5} One such application is germanium or silicon nanowire field-effect transistors (FETs) which have recently been reported to have high hole/electron mobilities, large on currents, large I_{ON}/I_{OFF} ratios, and good subthreshold swings.^{6–8} These novel transistors are attracting attention due to their potential applications in electronics and biomolecular detection. Furthermore, these nanowires can be assembled to make three-dimensional multifunctional electronics such as electromechanical and resistance-change memory devices based on the layer-by-layer assembly method.^{9,10}

Current strategies for producing higher aspect ratio nanowires have mainly made use of the vapor-liquid-solid (VLS) method which benefits from catalyst activation of one end of the nanowire.¹¹ Growth of nanowires via VLS often suffers from the requirements

of high temperature, special conditions, and complex procedures. In general, the size and aspect ratio distributions of these nanowires are difficult to control.¹² Solution growth of nanowires provides an alternative strategy for generating one-dimensional nanowires. In recent years, the solution-liquid-solid (SLS) method has proved to be a useful approach for producing semiconductor nanowires.^{13–15} This method has several advantages, including ease of control of the mean diameter, narrow diameter distributions, and a comparably low reaction temperature (<400 °C).^{13,16} However, this method also requires a catalyst activation step at the beginning of growth which is similar to the VLS method. Hydrothermal methods have been found to be more effective when compared to the low-temperature solution route for low-cost and large volume production of anisotropic nanocrystals.^{17–19} For example, Peng et al. employed ammonium as a complexing agent for cadmium ions to synthesize cadmium selenide (CdSe) nanocrystals through a hydrothermal method.²⁰ They found that at 180 °C mainly CdSe nanowires with diameters of 20–100 nm and lengths ranging from tens of nanometers to 1 μm were produced. However, this method has poor

* To whom correspondence should be addressed. E-mail: ymlam@ntu.edu.sg.

[†] Nanyang Technological University.

[‡] Technical University of Denmark.

- (1) Lu, W.; Lieber, C. M. *Nat. Mater.* **2007**, *6*, 841.
- (2) Tian, B.; Zheng, X.; Kempa, T. J.; Fang, Y.; Yu, N.; Yu, G.; Huang, J.; Lieber, C. M. *Nature* **2007**, *449*, 885.
- (3) Hu, Y.; Churchill, H. O. H.; Reilly, D. J.; Xiang, J.; Lieber, C. M.; Marcus, C. M. *Nat. Nanotechnol.* **2007**, *2*, 622.
- (4) Jiang, X.; Xiong, Q.; Nam, S.; Qian, F.; Li, Y.; Lieber, C. M. *Nano Lett.* **2007**, *7*, 3214.
- (5) Patolsky, F.; Timko, B. P.; Zheng, G.; Lieber, C. M. *MRS Bull.* **2007**, *32*, 142.
- (6) Liang, G.; Xiang, J.; Karche, N.; Klimeck, G.; Lieber, C. M.; Lundstrom, M. *Nano Lett.* **2007**, *7*, 642.
- (7) Cui, Y.; Zhong, Z.; Wang, D.; Wang, W. U.; Lieber, C. M. *Nano Lett.* **2003**, *3*, 149.
- (8) Li, Y.; Xiang, J.; Qian, F.; Gradecak, S.; Wu, Y.; Yan, H.; Blom, D. A.; Lieber, C. M. *Nano Lett.* **2006**, *6*, 1468.
- (9) Sapatnekar, S.; Nowka, K. *IEEE Des. Test Comput.* **2005**, *22*, 496.
- (10) Yu, G.; Cao, A.; Lieber, C. M. *Nat. Nanotechnol.* **2007**, *2*, 372.

- (11) Milliron, D. J.; Hughes, S. M.; Cui, Y.; Manna, L.; Li, J.; Wang, L. W.; Alivisatos, A. P. *Nature* **2004**, *430*, 190.
- (12) Holmes, J. D.; Johnston, K. P.; Doty, R. C.; Korgel, B. A. *Science* **2000**, *287*, 1471.
- (13) Sun, J.; Buhro, W. E. *Angew. Chem., Int. Ed.* **2008**, *47*, 3215.
- (14) Puthussery, J.; Lan, A.; Kosel, T. H.; Kuno, M. *ACS Nano* **2008**, *2*, 357.
- (15) Fanfair, D. D.; Korgel, B. A. *Chem. Mater.* **2007**, *19*, 4943.
- (16) Wang, F.; Dong, A.; Sun, J.; Tang, R.; Yu, H.; Buhro, W. E. *Inorg. Chem.* **2006**, *45*, 7511.
- (17) Cao, M. H.; Hu, C. W.; Peng, G.; Qi, Y.; Wang, E. J. *Am. Chem. Soc.* **2003**, *125*, 4982.
- (18) Nie, Q.; Yuan, Q.; Chen, W.; Xu, Z. J. *Cryst. Growth* **2004**, *265*, 420.
- (19) Xi, L. F.; Lam, Y. M.; Xu, Y. P.; Li, L. J. *J. Colloid Interface Sci.* **2008**, *320*, 491.
- (20) Peng, Q.; Dong, Y. J.; Deng, Z. X.; Li, Y. D. *Inorg. Chem.* **2002**, *41*, 5249.

control over the size and shape of the nanowires produced. Alivisatos et al. developed a high-temperature (around 300 °C), nonaqueous-based method using organometallic precursors to control the shapes of CdSe nanocrystals.²¹ This method can generate nearly monodisperse CdSe nanorods due to separation of the nucleation and growth stages. CdSe rods and tetrapods have also been prepared in a mixed surfactant system.^{22,23} This method has been not only used to synthesize CdS, CdSe, and CdTe nanocrystals but also extended to the synthesis of ZnS and ZnSe nanocrystals as well as core/shell rods (or dots) of CdSe/CdS/ZnS and quantum dot–quantum well structures.^{24,25} The crystal quality and control over the morphologies of the nanocrystals synthesized have made this method very important in the development of light-emitting diodes and solar cells.^{26,27} Very recently, Kang et al. reported their research on preparing CdS nanowires using tetradecylphosphonic acid (TDPA) as a ligand where they mainly studied the effect of temperature on the morphology of the nanowires.²⁸

Although nanorods have been prepared for close to 10 years using the hot coordinating method, only Kang et al. reported the successful synthesis of nanowires using a catalyst-free and solution-based synthesis method.²⁸ Catalyst-free, solution-based synthesis methods are much cheaper and easier to scale up to industrial proportions than other methods for synthesizing nanowires. In our systematic investigation of nanowire formation we determined the optimum parameters for synthesis by this method to maintain a good balance between nucleation and growth. These conditions favor formation of high aspect ratio nanocrystals.

As discussed earlier, solution synthesis methods are more commonly used to prepare nanostructures with low aspect ratio such as rods and dots. In this work, we report a general method to prepare very long monodisperse CdS nanowires using solution synthesis. As well as the reaction temperature, we also investigate the effect of the reactant ratio (ODPA-to-Cd mole ratio), the precursor ratio (Cd-to-S mole ratio), the precursor concentration, the precursor injection process, and the type of ligand on the morphology of the nanowires.

Experimental Section

Materials. TOPO (trioctylphosphine oxide, 99%) and poly(3-hexylthiophene) (P3HT) were purchased from Sigma-Aldrich. TOP (trioctylphosphine, 90%) and cadmium oxide (CdO, 99.95%) were purchased from Fluka. HPA (hexylphosphonic acid, 100%), DDDPA (dodecylphosphonic acid, 100%), ODDPA (octadecylphosphonic acid, 100%), and sulfur (99%) were purchased from Polycarbon Inc. and Chemicon.

Methods. The CdS nanowires were prepared using a modified Peng's procedure for cadmium chalcogen nanocrystals.²⁹ A 128 mg amount of CdO, 0.668 g of ODDPA (0.500 g of DDDPA or 0.232 g of HPA), and 3.00 g of TOPO were added to a 25 mL three-

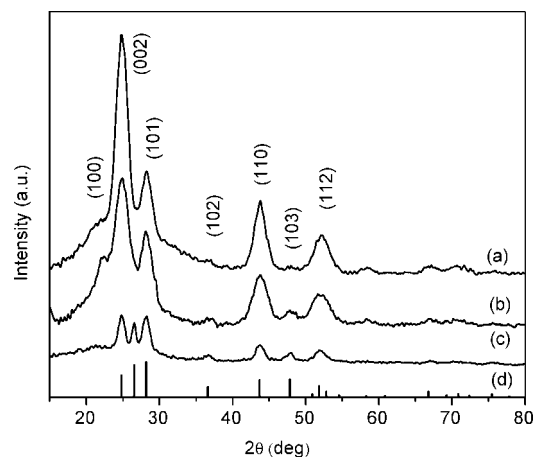


Figure 1. Typical XRD pattern of (a) 600 nm long as-prepared CdS nanowires, (b) shorter nanowires (150 nm in length), and (c) nanorods (14 nm in length) and (d) positions of the hexagonal CdS X-ray peaks (JCPDS).

neck flask equipped with a condenser and thermocouple adapter. The mixture was degassed at room temperature for 15 min. The flask was then filled with N₂, and the temperature was gradually raised to 330 °C to dissolve the CdO. After the CdO was dissolved and Cd complexes formed, the solution turned colorless. When the temperature was lowered to 310 °C, a solution of 32 mg of sulfur in 2.0 g of TOP was injected by multiple injections (4 times at 2 min intervals). After injection of sulfur, the temperature of the reaction mixture was maintained at 310 °C for further growth. The reaction was stopped by removing the heating mantle.

The procedure to clean the products was as follows: (1) the nanowires were initially purified by precipitating the particles with excess ethanol and discarding the supernatant after centrifuging twice. (2) The precipitate was then dispersed in the toluene. The solution obtained was centrifuged at 9500 rpm for 30 min. The precipitate that settled at the bottom of the tube was discarded. (3) The supernatant containing the nanowires was washed twice with toluene/ethanol and redissolved in toluene for further characterization and application.

TEM was carried out using a JEOL 2010 microscope fitted with a LaB₆ filament and an acceleration voltage of 200 kV. Ultraviolet–visible (UV–vis) absorption and photoluminescence (PL) spectra of the nanocrystals were obtained using a Shimadzu UV2501PC spectrophotometer and a Shimadzu RF-5301 PC fluorometer, respectively. The excitation wavelength for the PL test was 350 nm. Thin film X-ray diffraction (XRD) studies were carried out in a Rigaku DMAX 2200 using Cu K_α radiation.

Results and Discussion

Phase Analysis. Typical X-ray diffraction (XRD) patterns of the as-prepared CdS nanowires (600 nm in length), shorter nanowires (150 nm in length), and nanorods (14 nm in length) and the positions of the X-ray peaks for hexagonal CdS from the JCPDS are shown in Figure 1. All reflection peaks of the CdS nanocrystals, to within experimental error, can be indexed using hexagonal CdS (JCPDS card no. 41-1049). In addition, the strong and sharp (002) diffraction peak suggests that the crystalline domains are extended along the *c* axis. Comparison of XRD patterns for nanowires and nanorods reveals that the nanowires exhibit a sharper (002) peak compared to the rods due to their length. However, when comparing the XRD pattern of our CdS nanowires with

- (21) Peng, X. G.; Manna, L.; Yang, W. D.; Wickham, J.; Scher, E.; Kadavanich, A.; Alivisatos, A. P. *Nature* **2000**, *404*, 59.
 (22) Kanaras, A. G.; Sonnichsen, C.; Liu, H.; Alivisatos, A. P. *Nano Lett.* **2005**, *5*, 2164.
 (23) Manna, L.; Scher, E. C.; Alivisatos, A. P. *J. Am. Chem. Soc.* **2000**, *122*, 12700.
 (24) Manna, L.; Scher, E. C.; Li, L. S.; Alivisatos, A. P. *J. Am. Chem. Soc.* **2002**, *124*, 7136.
 (25) Battaglia, D.; Li, J. J.; Wang, Y.; Peng, X. *Angew. Chem., Int. Ed.* **2003**, *43*, 5035.
 (26) Coe, S.; Woo, W. K.; Bawendi, M.; Bulovic, V. *Nature* **2002**, *420*, 800.
 (27) Huynh, W. U.; Dittmer, J. J.; Alivisatos, A. P. *Science* **2002**, *295*, 2425.
 (28) Kang, C. C.; Lai, C. W.; Peng, H. C.; Shyue, J. J.; Chou, P. T. *Small* **2007**, *3*, 1882.
 (29) Peng, A. Z.; Peng, X. G. *J. Am. Chem. Soc.* **2002**, *124*, 3343.

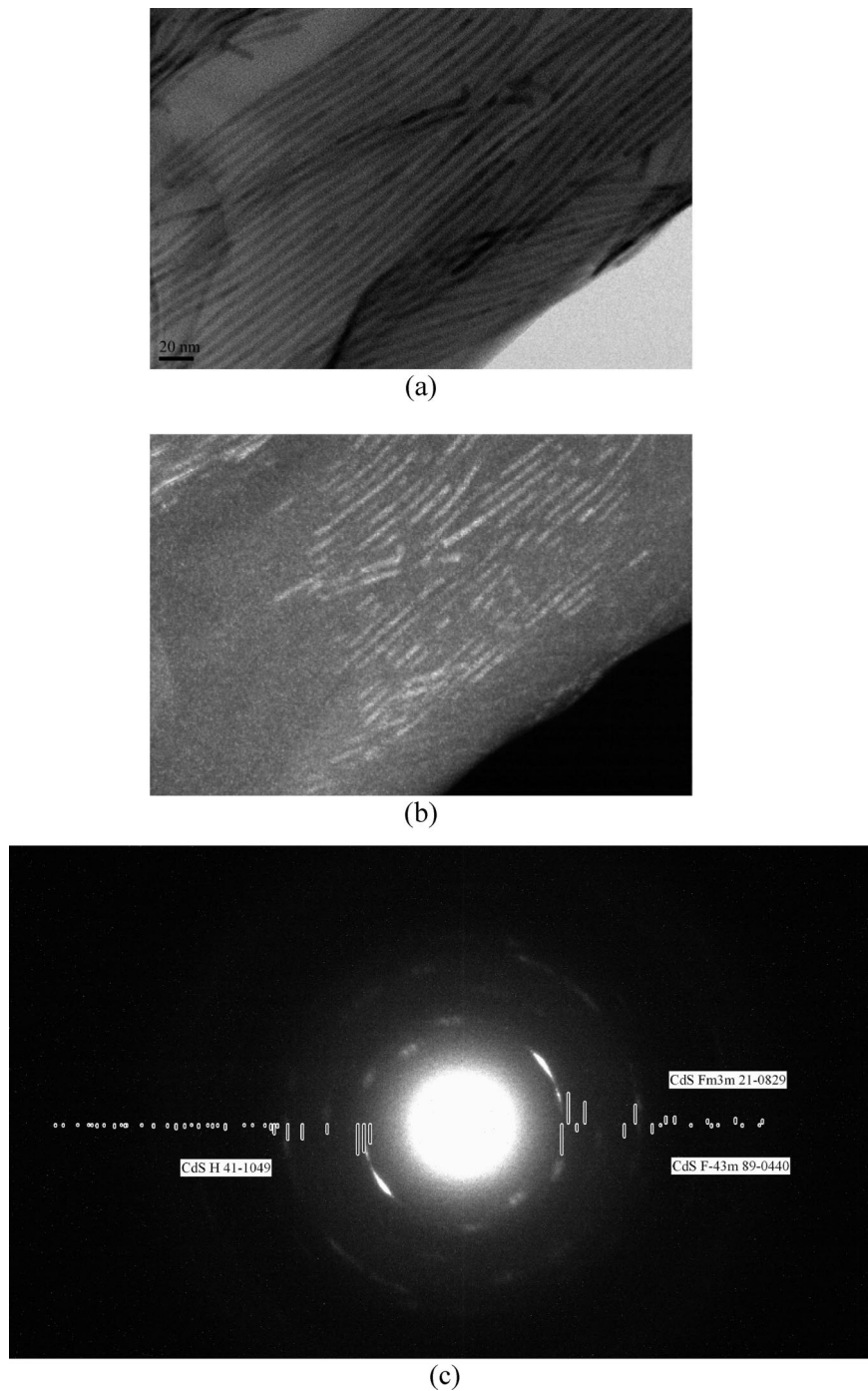


Figure 2. (a) Bright-field image of CdS nanowires, (b) dark-field image of the same CdS nanowires using the CdS 002 reflection, and (c) the diffraction pattern of the same area. The positions of the reflections for hexagonal CdS (CdS H JCPDS card no. 41-1049), cubic $Fm\bar{3}m$ CdS (21-0829) and cubic $F\bar{4}3m$ CdS (89-0440) are marked.

that of Kang et al.,²⁸ we found that our (002) peaks for both nanowires and nanorods are both more intense and sharper when compared to theirs. Our results are more reasonable in supporting the assumption that the nanowires grow along the c axis. This analysis is consistent with the results from other groups who synthesized CdS nanorods and nanowires.^{29–32} This growth orientation will be supported by high-resolution TEM and selected area electron diffraction studies discussed next. In contrast to the nanorods, the nanowires exhibit

several diffraction peaks with reduced intensity (particularly the (102) and (103) peaks). This is related to the fact that the nanowires readily self-assemble along certain directions and lie in the plane of the substrate during the XRD measurement process.

Bright-field and dark-field TEM images of the nanowires suspended on a holey carbon film are shown in Figure 2 along with a diffraction pattern of the same area. The bright-

(30) Yan, P.; Xie, Y.; Qian, Y.; Liu, X. *Chem. Commun.* **1999**, 1293.

(31) Bashouti, M.; Salalha, W.; Brumer, M.; Zussman, E.; Lifshitz, E. *ChemPhysChem* **2006**, *7*, 102.

(32) Long, Y. Z.; Chen, Z. J.; Wang, W. L.; Bai, F. L.; Jin, A. Z.; Gu, C. Z. *Appl. Phys. Lett.* **2005**, *86*, 153102.

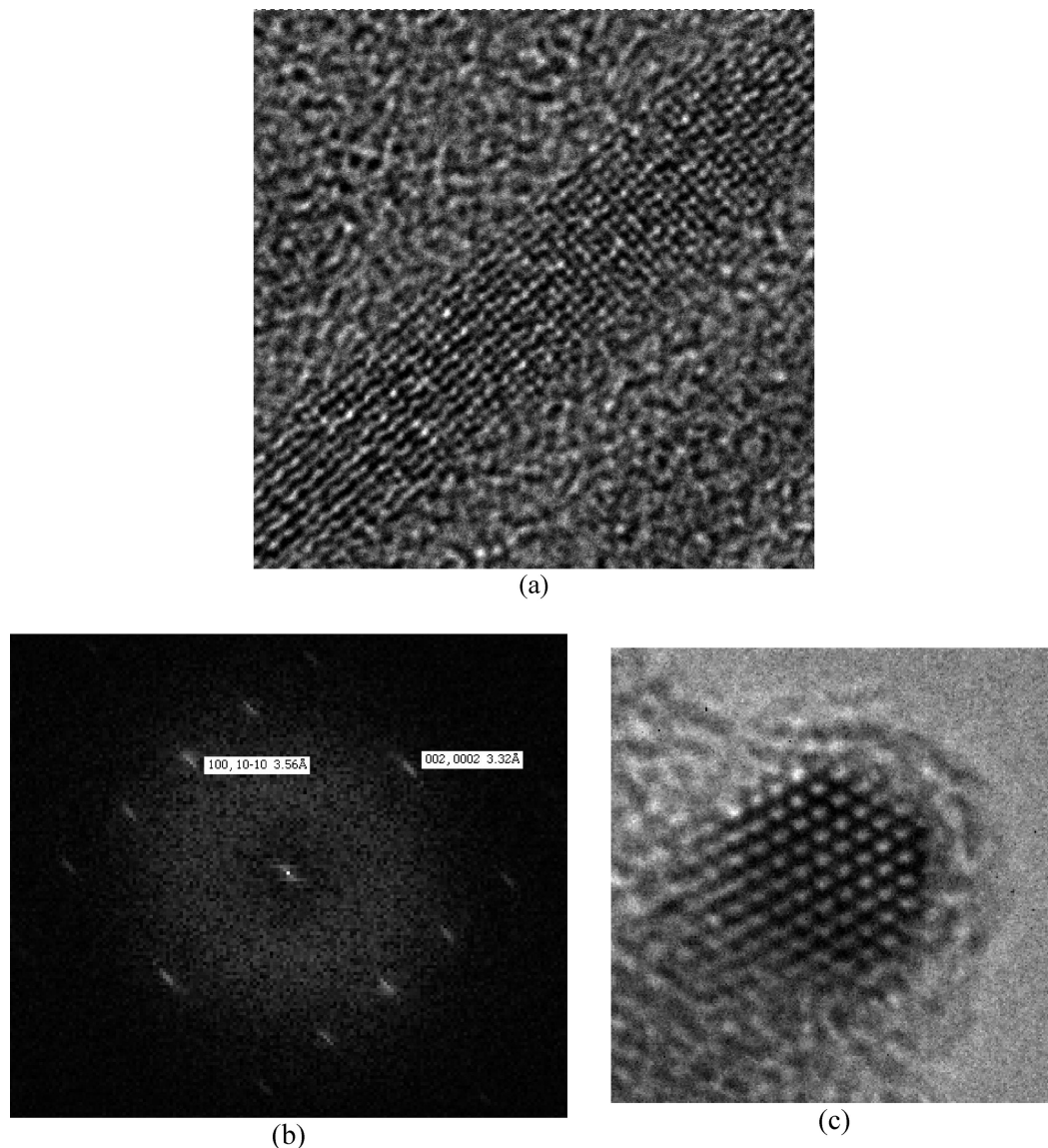


Figure 3. (a) High-resolution TEM image of a CdS nanowire, (b) FFT of the HRTEM image showing the indices, and (c) high-resolution image looking down the axis of a bent nanowire showing the hexagonal structure.

field image (Figure 2a) shows that the nanowires are long and have a uniform diameter. It can also be seen that they self-assemble into groups of parallel nanowires. The dark-field image (Figure 2b) was taken with the CdS 002 reflection and shows that the nanowires are mainly single crystal. The diffraction pattern (Figure 2c) shows the preferential orientation of the CdS nanowires with the strong 002 reflection along the length of the nanowires. The positions of the reflections for hexagonal CdS, cubic $Fm\bar{3}m$ CdS, and cubic $F\bar{4}3m$ CdS are marked, and it can be seen that the positions of the diffraction rings match those of hexagonal CdS, in agreement with the X-ray diffraction results of Figure 1a.

Figure 3a is a high-resolution image of one nanowire showing this region to be single crystalline with no stacking faults. The measured interplanar spacing of the lattice fringes along the length of the nanowire is about 0.332 nm, corresponding to the (002) lattice plane spacing of wurtzite CdS (0.336 nm). Figure 3b is a diffractogram from Figure

3a with spots marked corresponding to the 002 and 100 lattice fringes, indicating that the zone axis is [010]. Note the similarity between the diffractogram and the diffraction pattern from a group of nanowires shown in Figure 2c, indicating that the nanowires are all in similar orientations. A lattice image taken looking along the length of a nanowire at a point where the nanowire is bent is shown in Figure 3c. From this image the hexagonal structure of the nanowire is clear, confirming the [001] growth direction. All these results suggest that the CdS nanowires grow along the c direction with defect-free single crystals and that the crystal structure is the wurtzite CdS structure suggested by the XRD results discussed earlier.

Nanowire Morphology. 1. *Influence of the ODPA-to-Cd Mole Ratio.* In this study we found that the ligand-to-Cd mole ratio was a key factor that affects the morphology of the CdS nanocrystals in addition to the reaction temperature as found by other groups.²⁸ A series of experiments was performed with different ODPA-to-Cd mole ratios at fixed

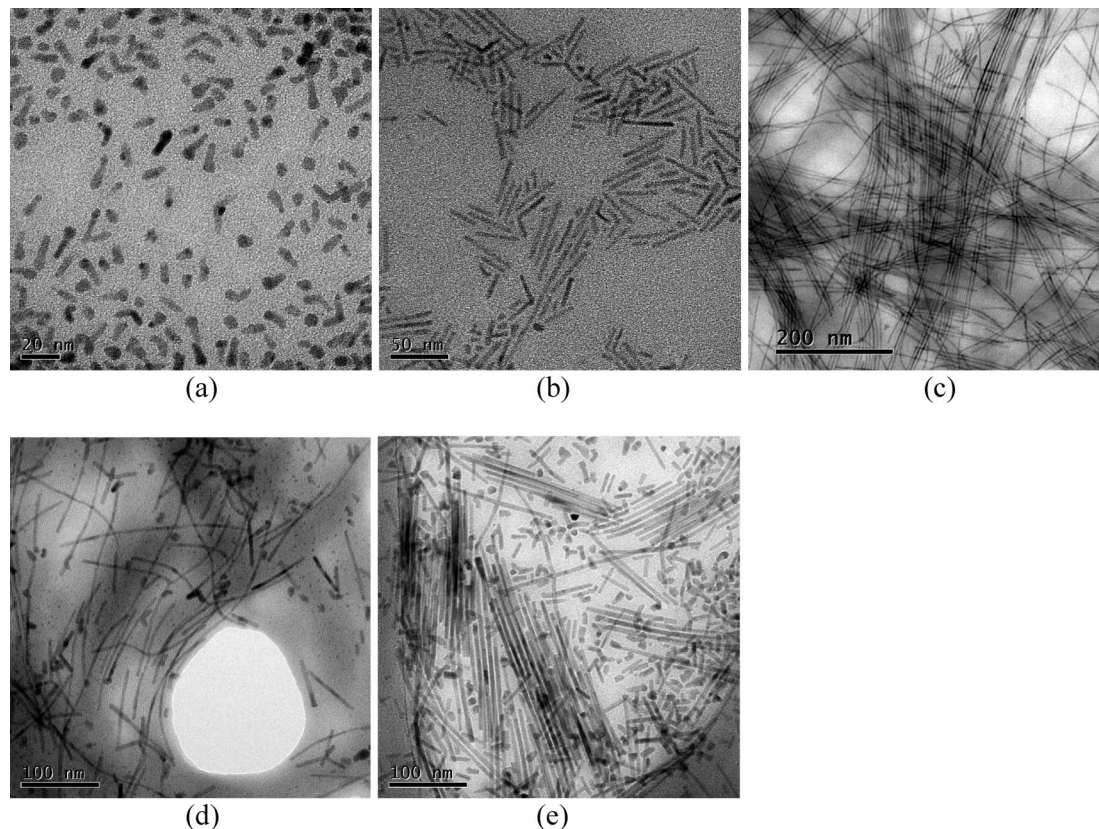


Figure 4. TEM images of CdS nanowires with ODPA-to-Cd mole ratios of (a) 1:1, (b) 1.5:1, (c) 2:1, (d) 3:1, and (e) 4:1.

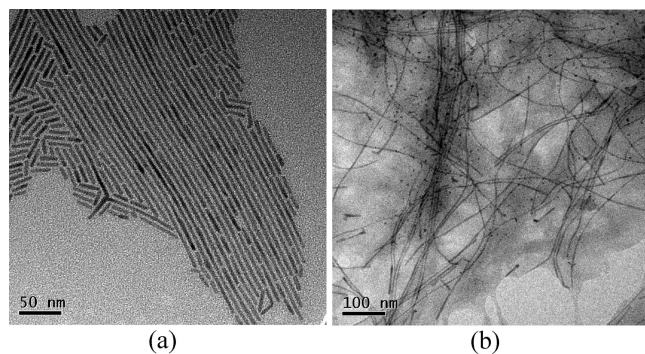


Figure 5. TEM micrographs of CdS nanowires synthesized with Cd-to-S mole ratios of (a) 1:1.5 and (b) 1:0.5.

initial concentration of Cd and Cd:S precursor ratio. If the ODPA-to-Cd mole ratio was less than 1, the solution would not turn colorless, indicating that the precursor has not completely decomposed. This was still the case even after holding the solution at 330 °C for more than 1 h. When the ODPA-to-Cd ratio was increased to 1:1, a mixture of short rods and dots (Figure 4a) was formed. The rods have a diameter of about 3.5 nm and length of about 15 nm. If the ratio was increased to greater than 1 but less than 2:1, the color of the Cd complex solution was lighter than when the ratio was 1:1, but still the solution did not turn totally colorless. The morphology of the nanocrystals synthesized was similar to that when the ratio was 1:1, but the length of the rods had increased to 40 nm while the diameter remained constant (Figure. 4b). When the ratio was increased to 2:1, the solution turned colorless after 20 min at 330 °C. The

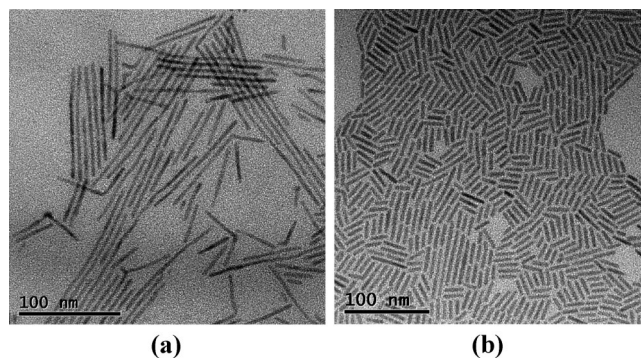


Figure 6. TEM images of CdS nanocrystals synthesized with (a) a single precursor injection and (b) multiple injections with an interval of greater than 5 min.

crystals formed were mainly nanowires with a monodisperse diameter of 3.5 nm, while their length had increased to 600 nm (Figure 4c). The general trend was that the aspect ratio increased as the ODPA-to-Cd mole ratio increased up to the mole ratio of 2:1, as shown in Figure 4a–c.

It was assumed by several groups that 2 mol of phosphonic acid is required to dissolve 1 mol of cadmium oxide (CdO) so that all the cadmium ions formed complexes with the phosphonic acid.^{33–35} A modified balanced chemical equation for this reaction is



Therefore, when the ODPA-to-Cd mole ratio is less than 2, CdO cannot be completely decomposed to form a colorless Cd complex solution at the reaction temperature. This results in a lower monomer concentration and hence decreases the

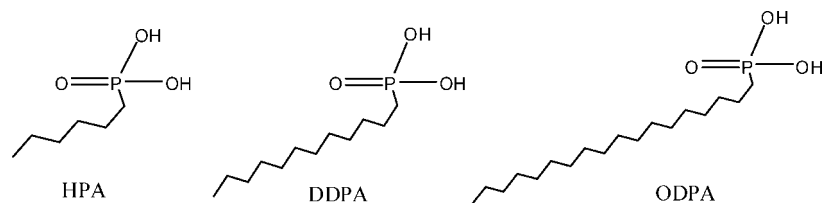


Figure 7. Chemical structures of three phosphonic acids with varying linear alkyl chain lengths.

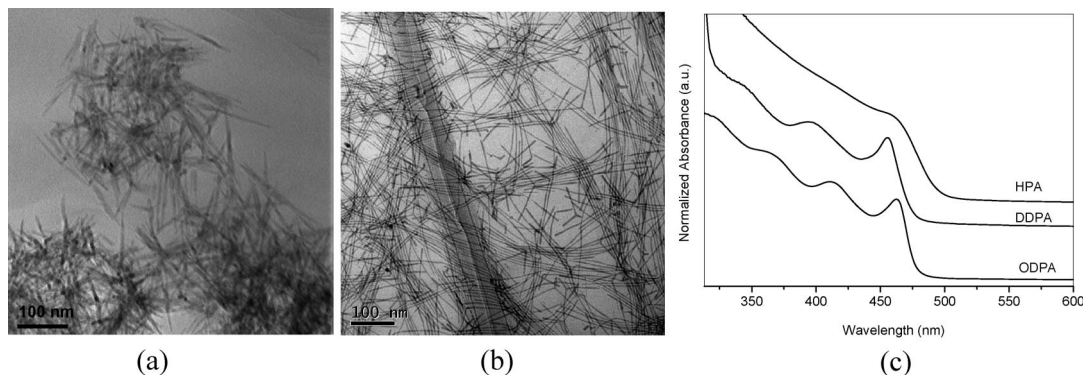


Figure 8. TEM micrographs of CdS nanocrystals synthesized with (a) HPA and (b) DDPA ligands. (c) UV-vis absorption spectra of nanocrystals produced with different ligands.

growth rate of the CdS nanocrystals. It is thought that anisotropic growth of the nanocrystals requires a high monomer concentration after the nucleation stage.²³ Therefore, we only get a mixture of short nanorods and dots when the ODPA-to-Cd mole ratio was equal to 1.5 (see Figure 4b). We noticed that Shieh et al. synthesized CdS, CdSe, and CdTe nanodots and nanorods with a mole ratio of TDPA-to-Cd equal to 1.73, which is close to 2 (there is an error in their calculation of the amount of TDPA in their supporting material).³⁶ They only managed to produce short nanorods (less than 100 nm) with a poor size distribution using a similar method. The main reason is possibly due to the mole ratio of TDPA-to-Cd that they used.

When the ODPA-to-Cd mole ratio was increased to 3, nanowires with different lengths ranging from 10 to 400 nm and a larger diameter of 3.7 nm were obtained as shown in Figure 4d. It was also found that the reaction speed was slower. If the mole ratio was further increased to 4, the reaction generated short nanowires mixed with a significant amount of short rods (Figure 4e). These nanowires had diameters of approximately 5 nm and lengths up to 300 nm. The length of the short rods ranged from 10 to 80 nm, while their diameter was roughly the same as the nanowires. The reaction speed was significantly slower. This observation is different from the results of Peng et al., where they studied the effect of the TDPA-to-Cd mole ratio on the morphology of CdSe nanocrystals.³³ They found that the growth rate of rods with a TDPA-to-cadmium ratio higher than 2 is significantly faster. In the synthesis of CdTe tetrapod-branch nanocrystals, Manna et al. thought that the presence of more

phosphonic acid per Cd decreases the reactivity of the Cd precursor and so the driving force for its addition to the crystal, leading to a slower growth rate for a given Cd concentration.³⁴

Recently, the Alivisatos group proposed that the concentration of phosphonic acid affects the cleavage of the alkylphosphine chalcogenide bond.³⁵ This process is supposed to result in formation of a semiconductor monomer, while the rate of this cleavage affects crystal nucleation and growth. We tentatively assume that the reason for the decreased reaction speed in our reactions is probably due to cadmium being more coordinated with ODPA and hence reducing the accessibility of the phosphine for the Cd. This leads to a reduction in the cleavage rate of the P=S double bond, leading to a relatively lower concentration of monomer and further affecting the nucleation and growth rate of anisotropic nanocrystals. Furthermore, we think that the rate at which P=S is broken is a vital factor affecting the morphology of nanocrystals in this system. We also attempted to synthesize CdSe nanowires using the same method, but we only managed to obtain nanorods with diameters of 10 nm and lengths of 40 nm. The reason for this is due to the faster cleavage rate of P=Se than P=S, which results in more nuclei and hence more rapid depletion of the monomers.³⁵ As a result, the rods had no more precursor to grow into nanowires.

2. Influence of the Cd-to-S Mole Ratio. The Cd-to-S mole ratio was another important factor that influenced the morphology of the resulting nanocrystals. It was found that decreasing the Cd-to-S mole ratio can lead to a decrease in the highest aspect ratio of the nanowires (see Figure 5a). A similar observation has been made by other groups.^{29,34} A possible explanation is that the more sulfur precursor present in the initial stage (lower Cd-to-S mole ratio), the faster the nucleation process occurs and more nuclei are formed during

(33) Peng, Z. A.; Peng, X. G. *J. Am. Chem. Soc.* **2001**, *123*, 1389.

(34) Manna, L.; Milliron, D. J.; Meisel, A.; Scher, E. C.; Alivisatos, A. P. *Nat. Mater.* **2003**, *2*, 382.

(35) Liu, H.; Owen, J. S.; Alivisatos, A. P. *J. Am. Chem. Soc.* **2007**, *129*, 305.

(36) Shieh, F.; Saunders, A. E.; Korgel, B. A. *J. Phys. Chem. B* **2005**, *109*, 8538.

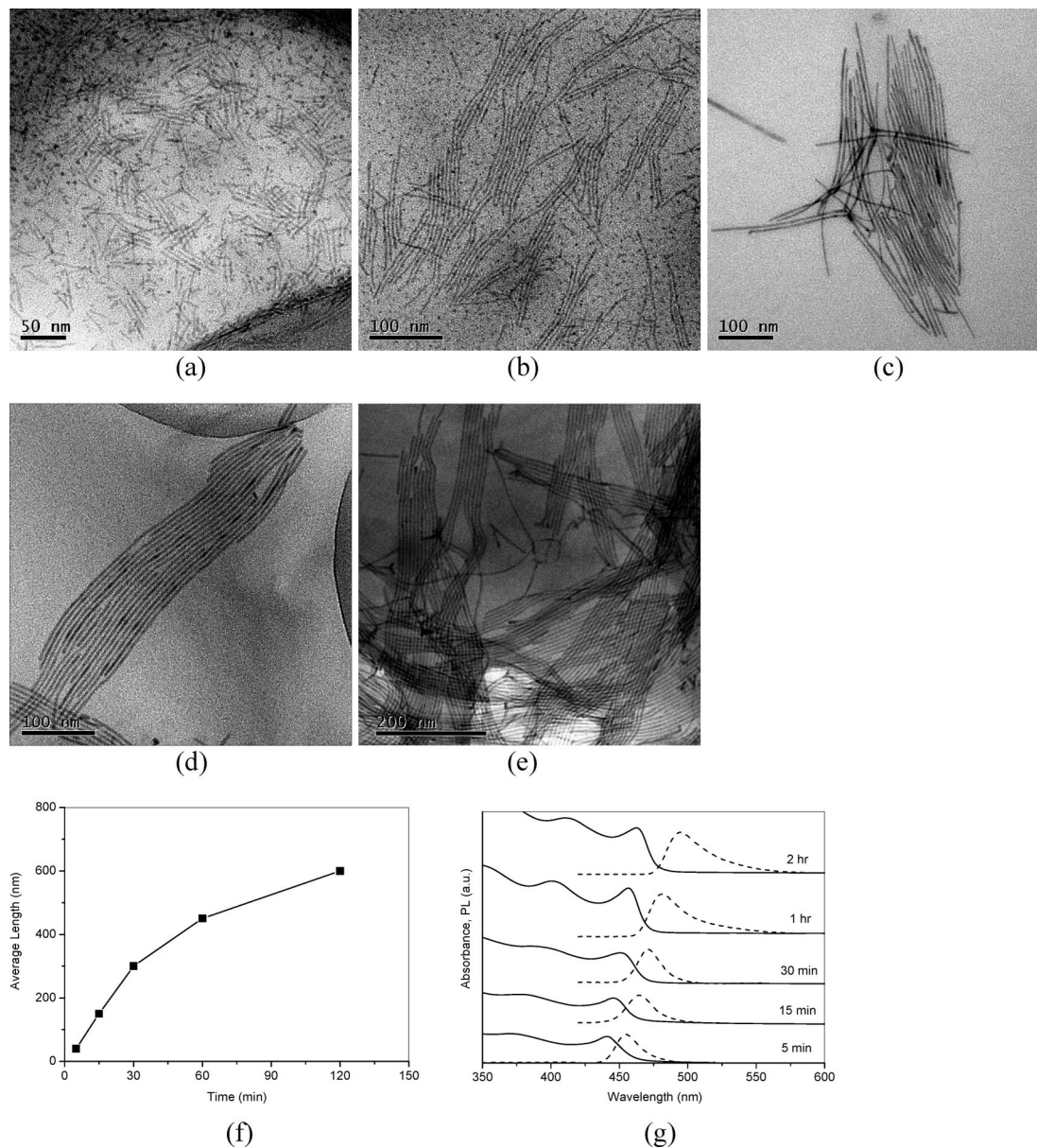


Figure 9. TEM images showing the temporal evolution of the CdS nanowires after (a) 5 min, (b) 15 min, (c) 30 min, (d) 1 h, and (e) 2 h. (f) Graph showing the change in the average length of the CdS nanowires over time. (g) UV-vis absorption (solid line) and PL emission spectrum (dotted line) of CdS nanowires obtained during nanowire growth.

nucleation. This results in a lower monomer concentration after nucleation.²⁹ This change is more significant as the Cd-to-S mole ratio is decreased further. However, anisotropic growth is due to the presence of a high monomer concentration after the nucleation stage.³⁷ The remaining low monomer concentration cannot sustain the anisotropic growth regime for a long time, resulting in a lower aspect ratio and a poor length distribution, ranging from 10 to 200 nm as shown in Figure 5a. When we increased the initial Cd-to-S mole ratio to 1:0.5, we obtained a mixture of tiny particles and nanowires with different lengths (see Figure 5b). This shows that these tiny particles are still in their early growth stage due to earlier depletion of the monomer which is limited by the amount of S.

3. Influence of the Precursor Concentration. The precursor concentration is another factor that influenced the morphol-

ogy of CdS nanowires. With the ODPA-to-Cd mole ratio fixed at 2:1 and the total amount of trioctylphosphine oxide (TOPO) and ODPA fixed at 3.668 g, changing the two precursor concentrations was found to change the morphology of the nanocrystals substantially. When the precursor concentration was reduced by one-half, shorter nanowires were produced. The length of the nanowires ranged from 50 to 150 nm, and the diameter was 3.4 nm. These results show that growth of longer nanowires requires a higher precursor concentration than growth of shorter ones.²⁹ When the precursor concentration is doubled, the reaction yields shorter nanowires mixed with short rods and dots. This result is not what we expected. In previous studies as the precursor concentration was increased, the morphology of the nanocrystals changed from spherical, short rods to long rods and then to branched rods.^{29,37} A higher precursor concentration may result in longer or branched nanowires. The reason for

(37) Peng, X. G. *Adv. Mater.* **2003**, *15*, 459.

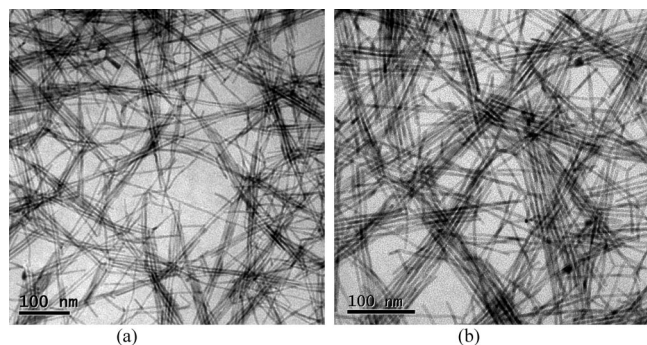


Figure 10. TEM images of the active layer of proposed hybrid solar cells with nanowire loadings of (a) 1:1 and (b) 1:3 by volume in a poly(3-hexythiophene) (P3HT) matrix.

formation of shorter nanowires mixed with short rods and dots at high concentration in our case may be due to the higher number of nuclei at the initial stage of the reaction. The speed of nucleation and growth is accelerated by increasing the precursor concentration.²⁹ These nuclei grow to larger crystals by consuming the semiconductor monomers.³⁵ With the depletion of the monomers, the final nanocrystals have different lengths.

4. Influence of the Precursor Injection Process. As discussed above, the monomer concentration at the initial stage of the reaction is an important factor because it can affect the rate of nucleation and growth. In this study, we investigated the effect of the precursor injection process on the morphology of the nanocrystals while keeping other parameters constant. It was found that a different final nanocrystal morphology was obtained when a single injection process was used instead of multiple injections. A single injection generates short, one-dimensional nanocrystals as shown in Figure 6a. Their length ranged from a few tens of nanometers to 200 nm, and their diameter was 3.7 nm. This is because the single injection introduced all the sulfur monomer at once, resulting in more nuclei during nucleation than for multiple injections. These nuclei consumed most of the monomer at the same time and hence led to a lower monomer concentration after nucleation. The remaining low monomer concentration cannot sustain the anisotropic growth regime for a long time, resulting in a lower aspect ratio as we discussed earlier. When multiple injections at 2 min intervals are carried out, the nanocrystals formed are nearly monodisperse nanowires with very high aspect ratios (refer to Figure 4c). We did not observe a significant difference in diameter between single and multiple injections that was reported by Peng et al.²⁹ They found a 1.8 nm difference in their experiments. The reason for the increase in aspect ratio using multiple injections is that multiple injections regularly replenish the monomer concentration and hence provide a relatively stable growth environment with high monomer concentration.^{21,29,33} In this case, after nucleation the presence of a high monomer concentration can maintain the anisotropic growth regime for a long time, resulting in a higher aspect ratio. Further increases of the interval between multiple injections can lead to a great decrease in the aspect ratio of the nanocrystals as shown in Figure 6b, where there is a mixture of nanorods with varying lengths but monodisperse diameter. Although these longer interval multiple

injections still periodically top up the available monomer, there is a variable growth environment and relatively low monomer concentration due to nucleation and growth between the longer intervals. This variable growth environment was not able to ensure anisotropic growth of the nanocrystals to high aspect ratio.

5. Influence of Different Ligands. We also investigated the effect of different ligands on the morphology of nanocrystals while keeping the other parameters constant. Three different phosphonic acids are used as ligands in the reaction, and their chemical structures are as shown in Figure 7. We found that the phosphonic acids with longer alkyl chains, such as octadecylphosphonic acid (ODPA), are better at controlling the morphology of the nanocrystals than those with shorter alkyl chains, such as dodecylphosphonic acid (DDPA) and hexylphosphonic acid (HPA).

It was found that the shorter alkyl chain phosphonic acid HPA can only generate nanoneedles with a rough surface. The diameter was around 7 nm and the length found around 150 nm. It can be seen that control of the morphology was poor as shown in Figure 8a. Using DDPA and ODPA, nanowires are formed mainly as shown in Figure 8b and Figure 4c, respectively. However, there is still a slight difference between these nanowires. Figure 8b shows that the morphology of the nanocrystals synthesized using DDPA is less well-controlled compare to those synthesized using ODPA. The product is a mixture of short rods, branches, and nanowires. The reason for the poor control over the nanocrystals morphology offered by phosphonic acids with shorter alkyl chains, such as HPA and DDPA, is due to the higher reactivity of the Cd–ligand complexes.²⁹ The reactivity of Cd–ligand complexes affects the P=S cleavage kinetics and nucleation/growth rate of anisotropic nanocrystals.³⁵ Furthermore, complexes with lower reactivity allow the monomers to adjust their position on the surface of the nanocrystal before binding occurs.²⁹ Therefore, Cd–ODPA complexes, which provide both a low diffusion rate and low reactivity, are good candidates for generating nearly monodisperse and high aspect ratio CdS nanowires. This may be the reason for the low monodispersity and varied morphology of CdS nanocrystals grown by Kang et al.²⁸

Figure 8c shows the UV–vis spectra of nanocrystals grown using HPA, DDPA, and ODPA ligands. The absence of a sharp peak in the spectrum from nanocrystals grown using HPA is due to the poor size distribution of the nanocrystals as shown in Figure 8a. The strong sharp peaks in the spectrum from nanocrystals grown using DDPA and ODPA indicate that their diameter is nearly monodisperse. The slight shift in the absorption peak from 456 nm for DDPA to 464 nm for ODPA grown nanocrystals indicates that the diameter of the nanowires has increased slightly.

6. Time-Dependent Shape Evolution Studies. To study the growth of these nanowires over time, aliquots were taken from the reaction flask at different times and examined in the TEM (Figure 9a–e). It is clearly seen that the length of the nanowires increased significantly while the diameter increased only slightly during the first 2 h of reaction (see Figure 9f). Tiny nanoclusters can be observed in Figure 9a

and 9b whose existence is an indication of the high monomer concentration present in the reaction.²⁹ A high monomer concentration supports 1D growth for formation of long nanowires. These nanoclusters gradually decrease as the reaction time is extended due to dissolution. However, some tiny clusters are still present even after 2 h. Apart from the nanowires, a small quantity of branched structures can also be seen in Figure 9a–e. These structures are often observed in the synthesis of II–VI anisotropic nanocrystals.^{23,29,33,36} This is because of the presence of multiple facets on the nucleating crystal that can grow at high monomer concentration.

Figure 9g shows the UV–vis absorption and PL spectra of the CdS nanowires during nanocrystal growth. It can be seen that the absorption band becomes sharper during the reaction, which indicates that the diameter remains fairly monodisperse throughout the growth. The slight shift in the absorption peak indicates that the diameter of the nanowires increased slightly during the reaction. As the nanowires grow longer, the long axis (length direction) grows beyond the confinement regime and the excitation peak only depends on the short axis (diameter) of the nanowires. This causes a red shift in the emission peak. The sharp and narrow peak in the PL spectra also indicates that the samples are monodisperse in diameter. With increasing reaction time, the PL peak shifts to a longer wavelength as the diameter of the CdS nanowires increases and becomes broader and less symmetrical due to near band-edge emission.

7. Potential Applications. A remarkable feature of the synthesis reported here is that the CdS nanowires exhibit a higher degree of dispersibility than nanorods of the same diameter. These highly dispersible nanowires have the potential to be processed into devices, such as solar cells and transistors, more readily. The nanowires can easily form an interconnected network in a conducting polymer thin film when prepared using spin coating. This is ideal for preparing the active layer of solar cells (see Figure 10a and 10b). It is thought that an active layer with a more intimate mixture can increase the amount of interaction between the conduct-

ing polymer chain and inorganic crystals.³⁸ This network structure can help exciton separation, diffusion of free charges, and charge collection efficiency.³⁹ In addition, nanowires with such small diameters (less than 5 nm) are ideal for fabrication of nanowire MOSFETs to study true one-dimensional transport at room temperature.⁶ Such MOSFETs provide a larger voltage margin to observe true one-dimension carrier conduction compared with larger diameter nanowires. Furthermore, these high-quality nanowires can be used as building blocks for memory and logic devices.^{1,9,10,40,41}

Conclusions

In summary, monodisperse CdS nanowires were successfully synthesized in solution. It was found that the mole ratio of ODPa-to-Cd is one key factor in determining the morphology of the CdS nanocrystals in addition to the reaction temperature. We also found that the precursor ratio (Cd-to-S mole ratio), the precursor concentration, and the precursor injection process can affect the morphology of the nanowires. In addition, it was found that Cd–ODPA complexes have both a low diffusion rate and a low reactivity compared to Cd–HPA or Cd–DDPA complexes. This makes ODPa a good candidate for generating nearly monodisperse and high aspect ratio nanowires. One remarkable feature of the CdS nanowires is their dispersibility. These highly dispersible CdS nanowires have the potential to be readily processed into devices, such as solar cells and transistors. Furthermore, our monodisperse nanowires could be aligned using an electric field or self-assembled in solution for nanoelectronic applications.

CM8014379

(38) Brabec, C. J. *Sol. Energy Mater. Sol. Cells* **2004**, *83*, 273.

(39) Hoppe, H.; Sariciftci, N. S. *J. Mater. Res.* **2004**, *19*, 1924.

(40) Patolsky, F.; Timko, B. P.; Yu, G.; Fang, Y.; Greytak, A. B.; Zheng, G.; Lieber, C. M. *Science* **2006**, *313*, 1100.

(41) Heath, J. R.; Kuekes, P. J.; Snider, G. S.; Williams, R. S. *Science* **1998**, *280*, 1716.